INTERNATIONAL JOURNAL OF CONSERVATION SCIENCE
ISSN: 2067-533X Volume 17, Issue 3, 2026: 1271-1286 www.ijcs.ro
DOI: 10. 36868/IJCS.2026.03.27

# ASSESSING WATER QUALITY FOR BLACK SEA ROMANIAN TRIBUTARIES AND COASTAL LAGOONS IN THE CONTEXT OF ARMED CONFLICT

Alexandra HARABAGIU[1,2], Maria CARACHICIU[1], Georgeta TUDOR[1,2], Monica MATEI[1,*], Mădălina BOBOC[1], Elena HOLBAN[1], Mirela FĂTU[1], Petrică VIZUREANU[3], Dumitru Doru BURDUHOS NERGIS[3], Andrei Victor SANDU[1,3,4], György DEÁK[1,2,4]

[1] National Institute for Research and Development in Environmental Protection 294 Splaiul Independenței Blvd, District 6, RO-060031, Bucharest, Romania
[2] Doctoral School Of Biotechnical Systems Engineering, National University of Science and Technology Politehnica of Bucharest, Splaiul Independenței 313, Bucharest, 060042, Romania
[3] Faculty of Material Science and Engineering, Gheorghe Asachi Technical University of Iași, 700050 Iași, Romania
[4] Academy of Romanian Scientists, Ilfov Street, no. 3, Bucharest, Romania

***Abstract***

*The overlap of armed conflict-related activities with industrial and domestic human actions is raising serious environmental concerns about potential contamination in the studied area and surrounding regions. This study assessed the quality of water and sediment quality in the Razim-Sinoe lagoon complex, as well as the Danube River mouths—Sulina, Sfântul Gheorghe, and the Chilia/Bystroe—located in close proximity to the conflict zone and the ecologically sensitive Danube Delta. Water and sediment samples were collected during field campaigns conducted between 2024 and 2025 and subsequently analyzed in the laboratory to determine physicochemical parameters. This pattern is likely driven by reduced biological activity, including denitrification and plant uptake, associated with lower temperatures and shorter daylight periods. Additionally, significant variations in heavy metal concentrations were detected in sediments, particularly for copper (Cu), nickel (Ni), lead (Pb), and zinc (Zn). Beyond the physicochemical assessment, the study integrates an evaluation of potential impacts on biodiversity and habitats, with particular attention to aquatic and coastal ecosystems influenced by the proximity to the Danube Delta, which may include alterations in species composition, habitat degradation, and increased ecological vulnerability due to contaminant exposure. The paper also examines forms of pollution directly associated with the armed conflict, particularly oil pollution affecting the marine ecosystem and the coastal zone, further exacerbating risks to biodiversity and ecological integrity. Based on these findings, several recommendations are proposed for the management and protection of affected areas for biodiversity conservation.*

***Keywords**: Black Sea biodiversity; Heavy metals; Pollution; Sediment quality; Water quality*

## Introduction

The quality of the water in the Black Sea is affected by pollution resulting from tributary river inflows, maritime activities (including transport, oil exploitation and military operations) and land-based military actions [1], [2], [3]. Surface water status is assessed based on the concentrations of several indicators, including dissolved nutrients (ammonium nitrogen, nitrite nitrogen, and orthophosphate), as well as total nitrogen and total phosphorus, which collectively contribute to the occurrence of eutrophication [4], [5], [6]. Marine water pollution is also generated by solid waste

[*] Corresponding author: monicamatei06@gmail.com

from ships and sinking military equipment that eventually corrodes and releases toxic substances into the aquatic environment. The most harmful pollutants resulting from warfare at sea include oil, which forms a film on the surface, and heavy metals such as lead, copper, cadmium, and mercury, as well as fuel compounds [7]-[10].

Heavy metals (HMs) are highly hazardous contaminants due to their persistence, toxicity, and bioaccumulation in aquatic plants (macrophytes), invertebrates, and fish, with further impact on humans through the food chain [11], [12], [13]. In aquatic and marine ecosystems, heavy metals are transported and dispersed by ocean currents and river flows, causing ecological impacts and endangering biodiversity [14], [15]. While the dispersion of pollutants may reduce their ecological impact at the local level, over time, bioaccumulation can have significant effects on terrestrial ecosystems, lagoons, and marine environments, impacting plants, invertebrates, and fish [16], [17].

The Black Sea coast ecosystem and its tributaries have been affected by armed conflict, oil spills, sea mines, and toxic substances carried by rivers from land-based military activities [18]. Despite the growing global focus on the environmental impact of armed conflicts, there is still a lack of comprehensive data on conflict-related pollution in this region [19]. This issue makes it challenging to create a viable long-term strategy for biodiversity conservation, including measures to protect the natural environment, in the coastal region and the Black Sea.

This study aims to address this knowledge gap by assessing physico-chemical parameters, heavy metal contamination, and oil spills (TPH analysis) in aquatic ecosystems potentially affected by armed conflicts. This will contribute to a better understanding of the ecological and environmental implications of these activities and the measures needed to conserve biodiversity. The seasonal dynamics of water pollutants in the Danube's lagoons and river mouths linked to the Black Sea have been relatively understudied. The objective of this paper is to assess the direct impact of the armed conflict on protected areas, taking into account the overlapping effect with the pollution from civilian activities.

This overlap is very important in the current geopolitical context because there is a high possibility that the cumulative effects will persist over time and have a major impact on the conservation of biodiversity in the coastal area.

## Materials and methods

### *Study area and sample sites*

This paper investigates the Razim-Sinoe lagoon complex and the Danube River mouths Sulina, Sfântul Gheorghe, and Chilia/Bystroe connected to the Black Sea to assess the impact of armed conflict-related activities combined with industrial and domestic human activities on water and sediment quality. To investigate seasonal variations, a total of 24 samples (12 water and 12 sediment) were collected during two distinct campaigns in autumn 2024 and summer 2025. The geographical coordinates of the sampling sites are detailed in Table 1, while their spatial distribution is illustrated in Figure 1.

**Table 1.** Geographical coordinates of the sampling sites for water and sediment (Autumn 2024 – Summer 2025)

| Sampling site | 2024 | Geographical Coordinates | Distance [km] | 2025 | Geographical Coordinates |
|---|---|---|---|---|---|
| **Razim 1** | Sample 1 | 28° 56' 41.7313" E<br>44° 43' 13.5863" N | 5.16 | Sample 7 | 28° 59' 17.7252" E<br>44° 41' 08.9520" N |
| **Razim 2** | Sample 2 | 29° 00' 08.2723" E<br>44° 49' 44.4894" N | 25.69 | Sample 8 | 28° 54' 48.7620" E<br>44° 36' 23.9040" N |
| **Razim 3** | Sample 3 | 29° 06' 50.1643" E<br>44° 47' 25.6043" N | 0.00 | Sample 9 | 29° 06' 50.1660" E<br>44° 47' 25.6056" N |
| **Sf. Gheorghe** | Sample 4 | 29° 37' 11.8939" E<br>44° 52' 43.1757" N | 1.45 | Sample 10 | 29° 36' 19.9620" E<br>44° 53' 12.1488" N |
| **Sulina** | Sample 5 | 29° 45' 06.5150" E<br>45° 09' 08.0229" N | 4.07 | Sample 11 | 29° 42' 12.7476" E<br>45° 09' 55.5984" N |
| **Chilia** | Sample 6 | 29° 44' 18.9855" E<br>45° 10' 24.3029" N | 16.22 | Sample 12 | 29° 40' 00.4728" E<br>45° 18' 37.0476" N |

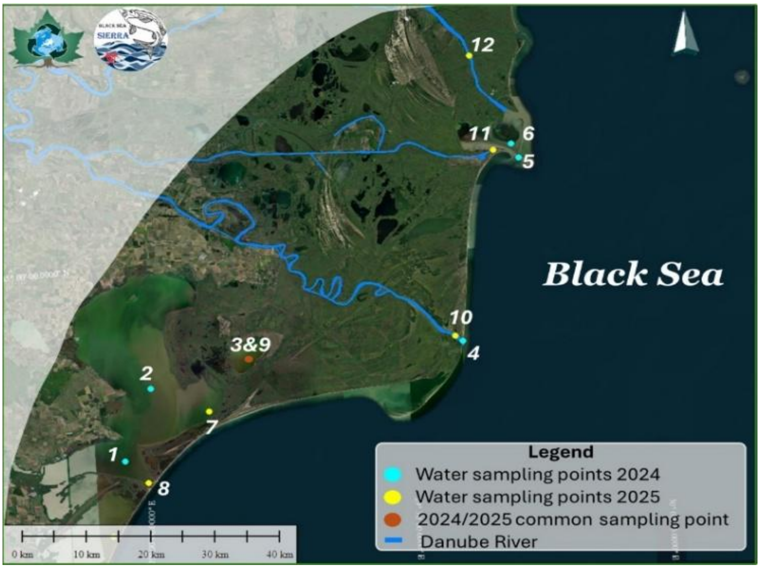


**Fig. 1.** Geographical distribution of the water (n=12) and sediment (n=12) sampling sites within the Razim-Sinoe lagoon complex and the Danube River mouths during the Autumn 2024 and Summer 2025 campaigns

***Water and sediment sampling methodology***

The sampling campaign conducted in autumn 2024 (Figures 2A and 2B) lasted 7 days and took place under lower temperature conditions (min. 9°C – max. 17°C), whereas the summer 2025 campaign (Figures 2C and 2D) lasted 5 days and was carried out during higher temperatures (min. 27°C – max. 29°C). All sampling procedures were carried out in accordance with fundamental principles that ensure the quality, representativeness, and traceability of data. Samples were collected by qualified personnel in accordance with standards (e.g., ISO 5667-1:2023; ISO 5667-3:2024; ISO 5667-19:2004; ISO 5667-12:2017). The samples were collected using a Kemmerer water sampler, ensuring that the collected water was representative of the in-situ conditions. The collected water samples were transferred to pre-cleaned polyethylene containers in accordance with international standards. Immediately after collection, the samples were stored under isothermal conditions (4-6°C) during transport to the laboratory in order to maintain their physical, chemical, and biological integrity until analysis.

The sediment sampling area was marked with transverse lines spaced 100 m apart, parallel to the coastline, and divided into three equally spaced intervals (nearshore, mid-beach, and upper beach). Sediment samples were collected in a 50 × 50 cm area, at a depth of 0–5 cm, using a metal shovel. Four samples from each corner of the delimited area were combined to form a composite sample weighing approximately 1000 g, representing the sampling area. Each sample was assigned a unique identification code to ensure traceability throughout all analytical stages.


**Fig. 2.** *In-situ* operations during the monitoring campaigns: A and B Autumn 2024 campaign; C and D Summer 2025 campaign

### *Analytical procedures/methods for physico-chemical characterization and heavy metal determination of water and sediment samples*

The physico-chemical analyses and the determination of heavy metal content were carried out in the laboratory according to the national standard methods. Firstly, pH and conductivity were measured with a WTW Multiparameter Benchtop Meter InoLab, while turbidity was measured with a portable turbidimeter (Velp Scientifica TB1). The selected water quality indicators, nutrients (nitrite nitrogen, nitrate nitrogen, and ammonium nitrogen), and chlorides were determined by using molecular spectrometry (VIS Jenway 6400) and titrimetric methods, respectively, following standard analytical procedures. The determination of the heavy metal concentrations was carried out by Flame Atomic Absorption Spectroscopy, using a ContrAA 700 HRCSAAS spectrometer (Analytik Jena, Germany), on water samples previously treated with concentrated $HNO_3$ (65%) to reach a concentration of 1% (v/v) in order to preserve dissolved metals. Total Petroleum Hydrocarbons (TPH) content in water was determined by the FTIR spectrophotometric method (FT/IR Jasco 4000) after extraction of petroleum products with $CCl_4$.

Sediment samples were dried in an oven at a temperature of 50–55°C to a constant mass, ground, and sieved using an Analysette 3 Spartan sieving system to obtain a homogeneous matrix. For the determination of heavy metal content, the sediment fraction $\leq 63$ µm was used. In order to dissolve the heavy metals, the sediment samples were digested with Aqua Regia ($HCl:HNO_3$ in a 3:1 ratio) using a microwave digestion method. Heavy metal concentrations were quantified by high-resolution atomic absorption spectrometry using a ContrAA 700 HRCSAAS spectrometer.

### *Satellite imagery and GIS analysis*

The analysis of oil pollution in the marine ecosystem resulting from the armed conflict was realized by radar satellite imagery downloaded from the Copernicus Browser platform [20]. To better visualize oil spills in the Black Sea, satellite images were adjusted, and corrections were applied using SNAP ESA [21]. After this, the data was mapped in QGIS using different parameters (the limits of protected areas and the localization of the oil spill) [22].

### *Statistical analysis and data visualization*

To analyze the spatiotemporal patterns of water quality parameters, including physico-chemical characteristics and heavy metal concentrations in both water and sediment samples, hierarchical clustering and heatmap visualizations were generated using the ClustVis platform [23]. The comprehensive dataset, comprising physico-chemical indicators (pH, conductivity, turbidity, $N\text{-}NO_2$, $N\text{-}NO_3$, $N\text{-}NH_4$, and chlorides) and trace elements (Cd, Cu, Ni, Pb, Zn, and Fe), was log-transformed using the $\ln(x + 1)$ function to normalize the distribution and ensure variance stability. To provide a robust overview of the environmental dynamics, two distinct scaling approaches were employed: first, unit variance scaling was applied to rows to highlight the relative dominance of specific parameters within each sampling site, and second, unit variance scaling was applied to columns to facilitate a direct comparison of values across the entire study area relative to the global mean. In all instances, hierarchical clustering was performed using Euclidean distance and Ward's linkage method to identify synergistic relationships between parameters and group sampling sites with similar environmental profiles.

The relationships between heavy metal concentrations (Ni, Cu, Pb, Zn, Fe) in sediments were evaluated using a staged statistical approach in Minitab version 22 [24]. Initially, the Pearson correlation coefficient (r) was employed to measure the intensity of linear associations. Subsequently, to validate these results in the presence of outliers and non-parametric distributions, the Spearman ($\rho$) correlation coefficient was calculated. To identify common sources and the structure of variance within the dataset, Principal Component Analysis (PCA) was applied [25]. Simultaneously, a separate statistical evaluation was conducted to determine the dynamics of Total Petroleum Hydrocarbons (TPH) specifically in relation to water quality. This assessment included physico-chemical parameters and heavy metal concentrations measured exclusively in the aqueous phase. Pearson and Spearman correlation coefficients were utilized to establish the degree of association between TPH and these waterborne constituents. Furthermore, a PCA was performed on the water-specific dataset to characterize the variance structure and to identify specific loading factors for TPH across the extracted principal components.

## Results and discussion

A total of 12 water samples and 12 sediment samples were collected during the monitoring campaigns, with six water and six sediment samples obtained in autumn 2024 and the remaining six water and six sediment samples collected in summer 2025. The physico-chemical characteristics of the water samples from the investigated sites, corresponding to each sampling campaign, are presented in Table 2.

As a key indicator of water quality, pH directly influences the chemical and biological processes within aquatic ecosystems. The impact of pH fluctuations on the physiology of marine and freshwater organisms is significant. Since species have evolved to thrive within specific pH ranges, any deviation can disrupt behavior, reproduction, and basic survival [26]. Similarly, elevated pH levels change the water's chemical composition, rendering the area uninhabitable. Although it is influenced by natural variations, water pH is heavily altered by human activities. Changes in pH affect the solubility and bioavailability of essential nutrients and pollutants; regulate biological processes such as nitrification, denitrification, and decomposition; and influence plant development [27], [28], [29]. Lower pH values trigger the release of toxic heavy metals from benthic sediments. This endangers both aquatic life and human health [30], [31]. According to the Romanian national legislation (Order No. 161/2006) [32], the acceptable pH range for surface waters is between 6.5 and 8.5, reflecting conditions suitable for maintaining ecological balance and supporting aquatic life. The same regulatory framework classifies water quality for physico-chemical parameters into five classes for nitrite ($N–NO_2$), nitrates ($N–NO_3$), and ammonium ($N–NH_4$). The concentration limits for $N–NO_2$ are 0.01 mg/L for Class I, 0.03 mg/L for Class II, and 0.06 mg/L for Class III. The concentration limits for $N–NO_3$ are classified with limits of 1 mg/L for Class I, 3 mg/L for Class II, and 5.6 mg/L for Class III, and for ammonium ($N–NH_4$), the thresholds are 0.4 mg/L for Class I, 0.8 mg/L for Class II, and 1.2 mg/L for Class III. These reference values were applied in the present study to evaluate the quality status of the investigated water samples. Surface water quality is classified into five classes based on chloride content: Class I ≤ 25 mg/L, Class II ≤ 50 mg/L, Class III ≤ 250 mg/L, Class IV ≤ 300 mg/L, and all above 300 are considered Class V. The observed variations in physico-chemical parameters among the sampling sites can be explained by differences in hydrological dynamics, seasonal temperature fluctuations (autumn: 13°C; summer: 28°C), and varying degrees of anthropogenic pressure, including potential disturbances associated with conflict-related activities. Such factors can influence the transport, dilution, and accumulation of contaminants within the aquatic system.

The integrated analysis reveals distinct spatial and temporal patterns in water quality through two complementary scaling approaches that highlight different aspects of the aquatic environment. By first applying row-wise scaling (Figure 3A), the unique chemical signature of each individual location is defined, revealing that the Razim lagoon complex maintains a stable and conservative mineralized profile while the Danube branches, such as Chilia and Sulina, exhibit more dynamic nutrient-driven fluctuations between 2024 and 2025. Conversely, the column-wise scaling (Figure 3B) emphasizes the intensity of specific parameters across all study sites, which highlights the consistently high pH levels and identifies the Razim complex as a primary hotspot for chlorides and turbidity relative to the fluvial stations. The hierarchical clustering analysis further demonstrated a clear separation between the lagoon and riverine systems, confirming the relatively homogeneous character of the Razim complex, while the Danube branches appeared more strongly influenced by seasonal variability and hydrological dynamics.

**Table 2.** Physico-chemical properties of water samples collected in autumn 2024 and summer 2025 from lagoons and river mouths from the tributaries of the Danube. The values shown in black correspond to Class I water quality, those in blue indicate Class II, and those in red represent Class III, while orange highlighting indicates Class V; additionally, values in yellow represent parameters, such as pH, that exceed specific quality thresholds, all according to the national legislation (Order 161/2006)

| Sampling site/Campaign | | Razim 1 | Razim 2 | Razim 3 | Sf. Gheorghe | Sulina | Chilia |
|---|---|---|---|---|---|---|---|
| pH | 2024 | 6,52 | 8,45 | 7,27 | 8,17 | 8,06 | 8,21 |
| | 2025 | 9,49 | 9,5 | 9,45 | 8,46 | 7,89 | 8,34 |
| Conductivity [mS/cm] | 2024 | 0,587 | 0,572 | 0,584 | 0,416 | 0,444 | 5,16 |
| | 2025 | 0,566 | 0,570 | 0,570 | 0,392 | 0,987 | 0,414 |
| Turbidity [NTU] | 2024 | 14,35 | 23,8 | 12,62 | 12,56 | 14,75 | 5,7 |
| | 2025 | 59,96 | 56,2 | 54,4 | 18,58 | 12,64 | 44,9 |
| $N\text{-}NO_2$ [mg/L] | 2024 | 0,004 | 0,005 | 0,003 | 0,007 | 0,006 | 0,004 |
| | 2025 | 0,002 | 0,004 | 0,002 | 0,028 | 0,028 | 0,025 |
| $N\text{-}NO_3$ [mg/L] | 2024 | 0,155 | 0,297 | 0,059 | 1,268 | 1,161 | 0,317 |
| | 2025 | 0,023 | 0,025 | 0,021 | 0,350 | 0,231 | 0,344 |
| $N\text{-}NH_4$ [mg/L] | 2024 | 0,093 | 0,088 | 0,092 | 0,032 | 0,039 | 0,155 |
| | 2025 | 0,120 | 0,116 | 0,120 | 0,022 | 0,006 | 0,032 |
| Chlorides [mg/L] | 2024 | 86,2 | 87,24 | 86,55 | 20,16 | 21,55 | 1536,3 |
| | 2025 | 103,06 | 101,09 | 100,81 | 17.410 | 195,17 | 25,550 |

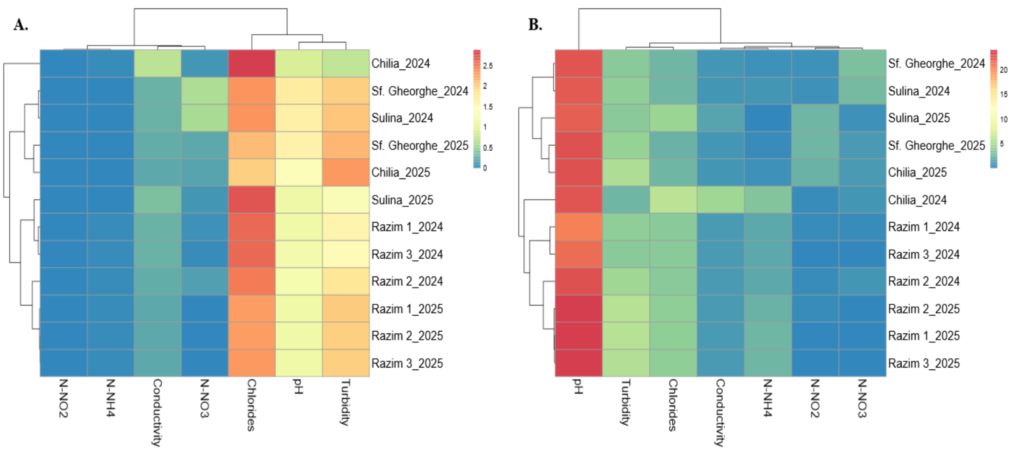


**Fig. 3.** Hierarchical clustering heatmaps illustrating the spatial and seasonal distribution of the physico-chemical parameters measured in surface water samples collected during the autumn 2024 and summer 2025 monitoring campaigns. A. Heatmap generated using ln(x + 1)-transformed data with unit variance scaling applied to rows. Both rows and columns were clustered using Euclidean distance and Ward's linkage method (12 rows, 7 columns); B. A heatmap was generated using ln(x + 1)-transformed data with unit variance scaling applied to columns. Both rows and columns were clustered using Euclidean distance and Ward's linkage method (12 rows, 7 columns)

***Heavy metal concentration of the water and sediment samples***

The analysis of heavy metals, including cadmium, copper, nickel, lead, zinc, and iron, was performed at all six sampling sites during both monitoring campaigns (autumn 2024 and summer 2025) in both surface water and sediment samples in order to assess their spatial distribution and potential ecological impact in the lagoon and river mouth environments. The results are summarized in Table 3. Surface water and sediment quality were evaluated in accordance with

Romanian national legislation (Order No. 161/2006), which establishes threshold values for classifying heavy metal concentrations. This framework served as a reference for interpreting the obtained results.

**Table 3.** Concentration of heavy metals [Cadmium (Cd), Copper (Cu), Nickel (Ni), Lead (Pb), Zinc (Zn), and Iron (Fe)] in water and sediment samples collected in autumn 2024 and summer 2025 from lagoons and river mouths from the tributaries of the Danube. The values shown in black correspond to Class I water quality, those in blue indicate Class II, while those highlighted in red represent Class III, and those in orange represent Class V according to the national legislation (Order 161/2006). Values highlighted in yellow represent concentrations that exceed the quality standards for sediments as established by national legislation (Order 161/2006)

| Sampling site/Campaign | | | Razim 1 | Razim 2 | Razim 3 | Sf. Gheorghe | Sulina | Chilia |
|---|---|---|---|---|---|---|---|---|
| **Water samples** | **Cd (µg/L)** | **2024** | *n.d.* | *n.d.* | *n.d.* | *n.d.* | *n.d.* | 0,25 |
| | | **2025** | *n.d.* | *n.d.* | *n.d.* | *n.d.* | *n.d.* | *n.d.* |
| | | **Trend** | ↔ | ↔ | ↔ | ↔ | ↔ | ↘ |
| | **Cu (µg/L)** | **2024** | 3,06 | 1,43 | 1,44 | 4,21 | 1,77 | 4,17 |
| | | **2025** | 3,725 | 1,683 | 1,003 | 0,758 | 2,723 | 2,747 |
| | | **Trend** | ↗ | ↗ | ↘ | ↘ | ↗ | ↘ |
| | **Ni (µg/L)** | **2024** | *n.d.* | *n.d.* | 0,32 | *n.d.* | *n.d.* | *n.d.* |
| | | **2025** | *n.d.* | *n.d.* | *n.d.* | *n.d.* | *n.d.* | *n.d.* |
| | | **Trend** | ↔ | ↔ | ↘ | ↔ | ↔ | ↔ |
| | **Pb (µg/L)** | **2024** | 0,09 | 3,2 | *n.d.* | 15,25 | 20,02 | 5,93 |
| | | **2025** | 10,970 | 7,403 | 5,754 | 3,57 | *n.d.* | 5,819 |
| | | **Trend** | ↗ | ↗ | ↗ | ↘ | ↘ | ↘ |
| | **Zn (µg/L)** | **2024** | *n.d.* | *n.d.* | *n.d.* | *n.d.* | *n.d.* | *n.d.* |
| | | **2025** | 3,021 | *n.d.* | 0,403 | *n.d.* | 0,016 | *n.d.* |
| | | **Trend** | ↗ | ↗ | ↗ | ↔ | ↗ | ↔ |
| | **Fe (µg/L)** | **2024** | *n.d.* | *n.d.* | *n.d.* | *n.d.* | *n.d.* | *n.d.* |
| | | **2025** | 0,257 | 7,194 | *n.d.* | 3,913 | 0,549 | 7,710 |
| | | **Trend** | ↗ | ↗ | ↔ | ↗ | ↗ | ↗ |
| **Sediment samples** | **Cd (mg/kg dry mass)** | **2024** | *n.d.* | *n.d.* | *n.d.* | *n.d.* | *n.d.* | *n.d.* |
| | | **2025** | *n.d.* | *n.d.* | *n.d.* | *n.d.* | *n.d.* | *n.d.* |
| | | **Trend** | ↔ | ↔ | ↔ | ↔ | ↔ | ↔ |
| | **Cu (mg/kg dry mass)** | **2024** | 1,09 | 1,41 | 1,30 | 1.28 | 2,66 | 1,96 |
| | | **2025** | 2,61 | 1,33 | 1,63 | 16,71 | 2,45 | 30,09 |
| | | **Trend** | ↗ | ↘ | ↗ | ↗ | ↘ | ↗ |
| | **Ni (mg/kg dry mass)** | **2024** | 5,69 | 7,37 | 6,63 | 12,14 | 9,670 | 10,61 |
| | | **2025** | 15,39 | 10,55 | 22,84 | 28,21 | 13,46 | 47,83 |
| | | **Trend** | ↗ | ↗ | ↗ | ↗ | ↗ | ↗ |
| | **Pb (mg/kg dry mass)** | **2024** | 3,56 | 4,02 | 3,10 | 2,84 | 2,47 | 4,21 |
| | | **2025** | 1,66 | 2,26 | 4,13 | 6,98 | 4,13 | 16,21 |
| | | **Trend** | ↘ | ↘ | ↗ | ↗ | ↗ | ↗ |
| | **Zn (mg/kg dry mass)** | **2024** | 12,37 | 14,13 | 12,6 | 13,13 | 17,55 | 19,69 |
| | | **2025** | 20,07 | 11,00 | 22,26 | 52,98 | 22,26 | 78,93 |
| | | **Trend** | ↗ | ↘ | ↗ | ↗ | ↗ | ↗ |
| | **Fe (mg/kg dry mass)** | **2024** | 6.049,99 | 6.015,12 | 5.946,96 | 5.787,32 | 7.267,02 | 6.654,00 |
| | | **2025** | 6.764,43 | 4.526,67 | 3.243,62 | 14.183,34 | 3.243,62 | 33.296,86 |
| | | **Trend** | ↗ | ↘ | ↘ | ↗ | ↘ | ↗ |

The analysis of the results presented in Table 3 indicates the absence of contamination by cadmium, copper, zinc, or nickel in the surface water samples collected from both the lagoon area and the Danube River mouths. In contrast, lead pollution is observed in the lagoon area during the summer and at the river mouths. Moreover, significant iron pollution is recorded at river mouths during the summer. Thus, based on the lead and iron results, the water falls under Level II Water Quality Standards for rivers and lakes, according to the Regulation on the Classification of Surface Water Quality for Determining the Ecological Status of Water Bodies (No. 161/2006). At the same time, it can be observed that pollution levels in the lagoons are lower than those at the Danube River mouths. Potential sources of water pollution with heavy metals include industrial discharges and former or ongoing military activities in the neighboring region [33], [34]. For example, the presence of remaining parts of explosives in the Black Sea and the connected freshwater can influence the water quality with an impact on both humans and marine ecosystems [35], [36]. The study conducted by Litynska M.I. and Pelekhata O.B. in 2024 regarding the heavy metals in some rivers in Ukraine showed a significant increase in concentrations of Cu, Pb, Cr, and Ni [37].

Figure 4 illustrates the spatio-temporal variation of heavy metal concentrations in sediments collected from the Razim–Sinoe lagoon complex and Danube River mouths during 2024–2025. The concentrations are presented as natural logarithm values, allowing comparison between locations and years for each analyzed metal: Cu (A), Ni (B), Pb (C), Zn (D), and Fe (E).

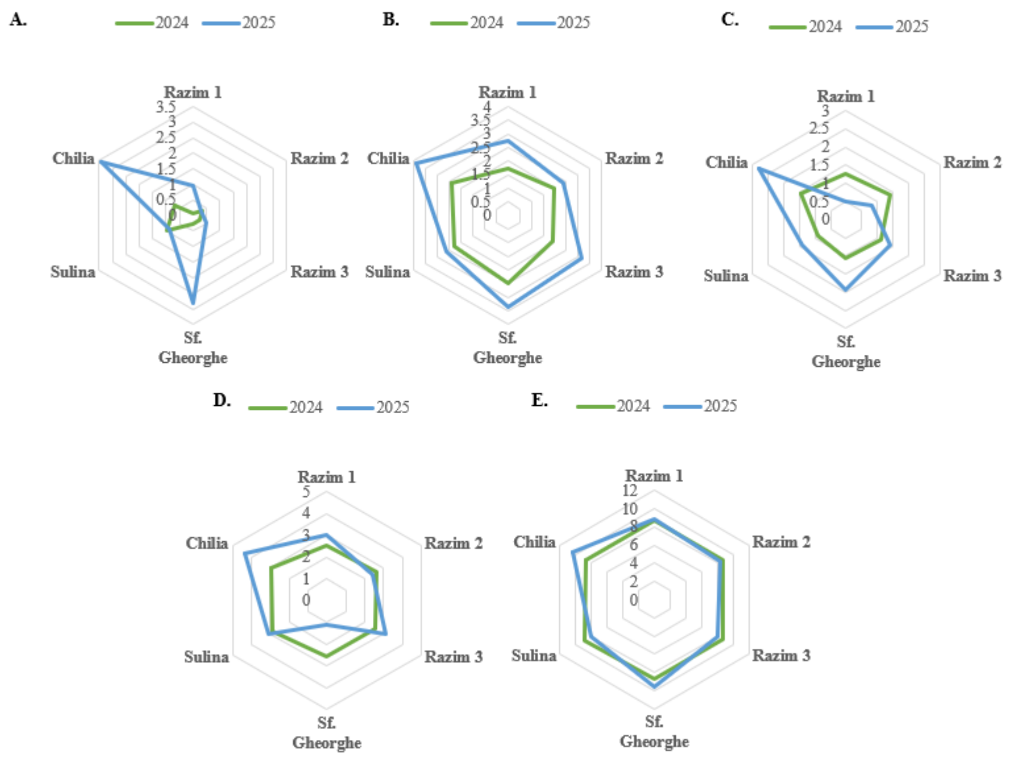


**Fig. 4.** Spatio-temporal distribution of heavy metal concentrations in sediments across sampling locations, expressed as natural logarithm values for the period 2024–2025: A is Cu, B is Ni, C is Pb, D is Zn, and E is Fe

The multivariate analysis of heavy metals in surface water samples revealed a heterogeneous distribution pattern, with lead (Pb) and copper (Cu) emerging as the main drivers of chemical variability. The row-wise scaling approach (Figure 5A) allowed the identification of site-specific metallic fingerprints. This visualization indicated that, during the 2024 campaign, the Sulina and Sf. Gheorghe branches were mainly characterized by a Pb-dominated signature. In contrast, the upper portion of the heatmap highlighted stations such as Sulina 2025 and Razim 1 and 3 (2024), which exhibited a profile primarily influenced by Cu, independent of the absolute concentrations of other elements in the dataset. The column-wise scaling approach (Figure 5B) provided a clearer representation of relative concentration gradients and potential pollution hotspots. This analysis identified Sulina 2024 as the most pronounced hotspot for Pb contamination, exhibiting the highest relative intensity within the Pb distribution. Similarly, elevated Cu levels were observed at the Chilia 2024 and Razim 1 (2025) stations, which appeared as major contributors to Cu variability across the study area. A noticeable temporal shift was observed within the Razim system, where samples from 2024 (Razim 2 and 3) showed comparatively lower metal enrichment, whereas the 2025 campaign indicated increased clustering associated with higher Cu and Zn levels. In contrast, Cd and Ni exhibited relatively stable distributions across most sampling sites, with only minor localized enrichments, such as Cd at Chilia 2024, which did not indicate widespread contamination during the study period. Overall, the combined analyses suggest that the 2024 campaign was characterized by localized Pb pressure in the main Danube branches, while the 2025 campaign reflected a more spatially restricted accumulation of trace metals within the Razim lagoon system. The hierarchical clustering of sediment data reveals a distinct geochemical behavior compared to the water column. According to the row-scaled analysis (Figure 5C), Iron (Fe) constitutes the dominant matrix across all samples, showing a strong synergistic relationship with Ni and Zn, which points toward a primarily geogenic origin. However, the column-scaled heatmap (Figure 5D) uncovers a significant temporal trend: the 2025 campaign, particularly in the Chilia and Sf. Gheorghe branches, exhibited substantially higher accumulation levels for Ni, Zn, and Fe compared to 2024. This shift suggests that while the riverine branches act as primary transport routes, they also function as active depositional environments for trace elements, with the Razim Lake system showing localized copper and lead enrichment in 2025.

Following the statistical processing of the sediment samples, a complex relationship between the analyzed heavy metals was observed. The integration of bivariate correlations and multivariate techniques allowed for a clear differentiation between localized contamination events and systemic geochemical trends. Initial results obtained through the Pearson test (Table 4, Figure 6A) indicated extremely strong positive correlations between all elements, with r values frequently exceeding 0.90, such as 0.969 for Fe-Cu and 0.951 for Fe-Pb. However, scatterplot analysis and the application of the Spearman coefficient (Table 4, Figure 6B) demonstrated that these values were heavily influenced by a single sampling point with anomalous concentrations, specifically station Chilia_2025. Using the Spearman method, which is more robust to outliers, a significant decrease in correlations was observed across most metals. The only resilient association was the Ni-Cu pair ($\rho = 0.706$), suggesting a common pollution source or similar geochemical behavior for nickel and copper across the study area. In contrast, the correlation between Zn and Fe dropped to a near-zero value ($\rho = -0.018$), indicating that zinc distribution is independent of iron oxide control in the majority of the sampled locations. The PCA analysis (Table 5) confirmed this distribution, with the first principal component (PC1) explaining 90.4% of the total variance. This dominance is clearly illustrated in the Score Plot (Figure 6C), where the sampling locations are discriminated based on their metal loading. Two distinct outliers are identified that deviate from the main cluster of stations: Chilia_2025 appears as an extreme outlier on the far right of the PC1 axis, representing a significant pollution hotspot with the highest overall metal concentrations; Sf. Gheorghe_2025 is positioned in the upper quadrant of the plot, showing a separation along the PC2 axis. This suggests a different compositional profile, likely driven by its specific copper (Cu) and iron (Fe) ratios. The Loading Plot (Figure 6D) complements these findings by highlighting the distinct positioning of Zn on the PC2 axis with a negative loading of -0.859, confirming its relative independence from the Ni-Cu-Pb-Fe cluster. The spatial separation shown in the Score Plot, combined with the vector orientations in the Loading Plot, confirms that the previously observed high correlations are primarily driven by localized extreme events in these specific river arms rather than by a uniform trend across the entire study area.

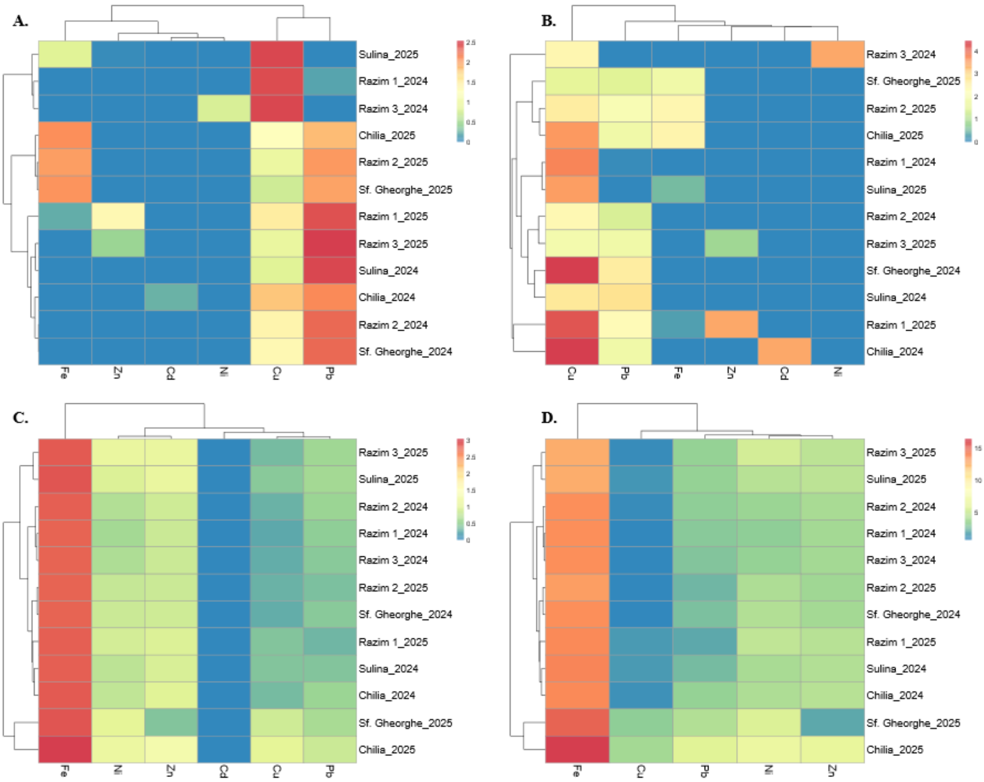


**Fig. 5.** Hierarchical clustering heatmaps illustrating the spatial and seasonal distribution of heavy metal concentrations in surface water and sediment samples collected during the autumn 2024 and summer 2025 monitoring campaigns. A. Surface water samples: heatmap generated using ln(x + 1)-transformed data with unit variance scaling applied to rows. Both rows and columns were clustered using Euclidean distance and Ward's linkage method (12 rows, 7 columns). B. Surface water samples: a heatmap was generated using ln(x + 1)-transformed data with unit variance scaling applied to columns. Both rows and columns were clustered using Euclidean distance and Ward's linkage method (12 rows, 7 columns). C. Sediment samples: a heatmap was generated using ln(x + 1)-transformed data with unit-variance scaling applied to the rows. Both rows and columns were clustered using Euclidean distance and Ward's linkage method (12 rows, 7 columns). D. Sediment samples: heatmap generated using ln(x + 1)-transformed data with unit variance scaling applied to columns. Both rows and columns were clustered using Euclidean distance and Ward's linkage method (12 rows, 7 columns)

**Table 4.** Pearson and Spearman correlation matrices for heavy metals in sediment samples

| | | Ni | Cu | Pb | Zn | | Ni | Cu | Pb | Zn |
|---|---|---|---|---|---|---|---|---|---|---|
| **Pearson Correlation** | **Cu** | 0.930 | | | | **Spearman Correlation** | 0.706 | | | |
| | **Pb** | 0.898 | 0.950 | | | | 0.469 | 0.406 | | |
| | **Zn** | 0.774 | 0.748 | 0.855 | | | 0.476 | 0.455 | 0.284 | |
| | **Fe** | 0.874 | 0.969 | 0.951 | 0.831 | | 0.224 | 0.616 | 0.235 | -0.018 |

**Table 5.** Eigenanalysis of the Correlation Matrix

| | | | | | |
|---|---|---|---|---|---|
| **Eigenvalue** | 4.5186 | 0.2958 | 0.1342 | 0.0461 | 0.0054 |
| **Proportion** | 0.904 | 0.059 | 0.027 | 0.009 | 0.001 |
| **Cumulative** | 0.904 | 0.963 | 0.990 | 0.999 | 1.000 |

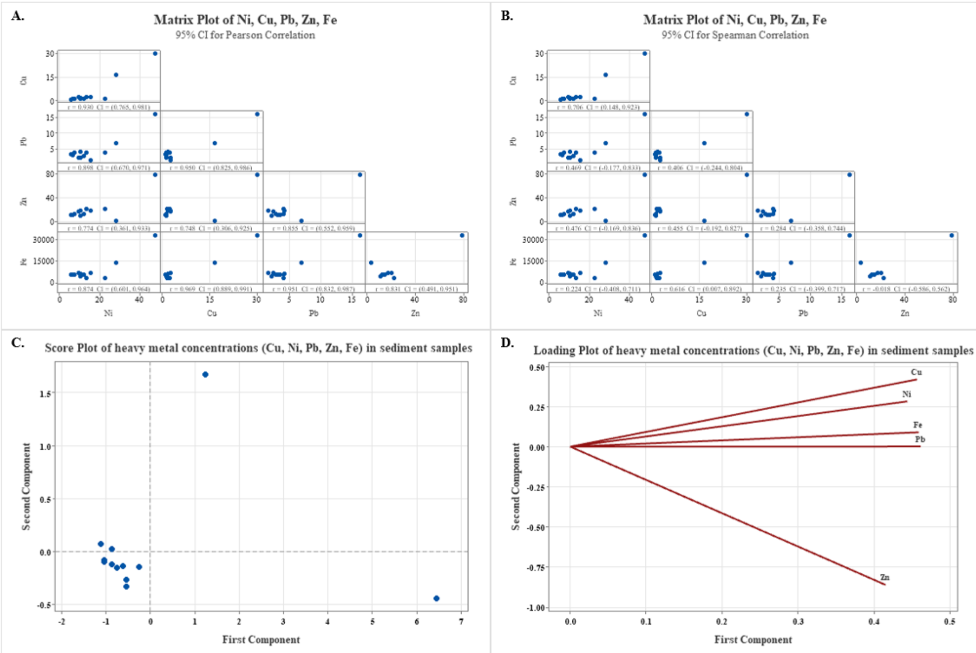


**Fig. 6.** Statistical and multivariate analysis of heavy metals in sediment samples. A. Matrix plot of Pearson correlation coefficients. B. Matrix plot of Spearman ρ correlation coefficients. C. PCA Score Plot: Displays the spatial distribution of sampling stations. The primary axis (First Component) identifies Chilia_2025 as a high-magnitude outlier, while the vertical axis (Second Component) isolates Sf. Gheorghe_2025 based on its distinct compositional profile. D. PCA Loading Plot: Visualizes the contribution of each metal to the principal components. The clustering of Cu, Ni, Fe, and Pb indicates a common geochemical driver, while the separation of Zn reflects its unique distribution pattern within the studied ecosystem.

## Oil pollution of the marine ecosystem due to armed conflict

Coastal and marine ecosystems have been severely impacted by chemical pollution from both land and sea. Furthermore, the environmental impact is intensified by increased wastewater discharges resulting from physical damage and power failures caused by military conflict [38]. Sunken military equipment adds vast quantities of toxic petroleum products, such as diesel, petrol, oils and greases, to the sea. These complex hydrocarbon mixtures spread across the surface of the sea, forming large oil slicks. Light fractions evaporate by approximately 25% within days, while low-molecular-weight components dissolve into the water column. Over time, these oil products undergo processes such as emulsification, oxidation and sedimentation, and are often consumed by marine organisms. A significant factor is the expansiveness of these oil films, which can trap and concentrate other hazardous pollutants such as heavy metals and pesticides [19], [39]. Another significant issue is the pollution caused by the sinking of warships or tankers, which adds to the pollution from civilian transport activities [40], [41]. The map highlights changes in the position and dispersion trends of the oil spills, and the overlay of marine current vectors facilitates the interpretation of transport directions and their dynamics over the analyzed period. At the same time, Figure 7 shows the overlap of the oil spills with two marine protected areas in Romania that were directly affected by the oil spill.

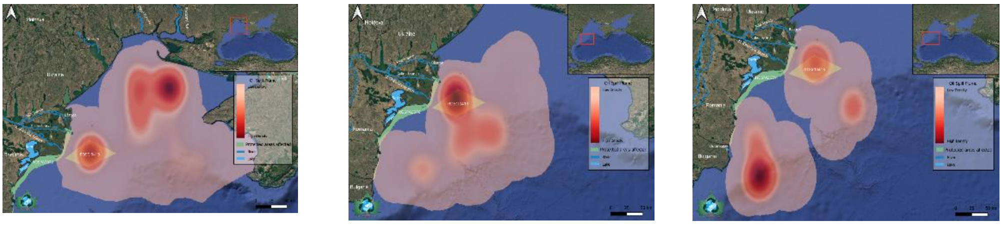

A. B. C.

**Fig. 7.** Detailed map of oil spills from: A December 2024 - January 2025. B February 2025. C March 2025

The oil spill has a direct impact on the ROSCI0413 protected area within 14 days of the event occurring, which, due to marine currents, can reach the Romanian or Bulgarian coast and, implicitly, the Razim-Sinoe lagoon.

Taking into account this situation/possibility, the total petroleum hydrocarbons (TPH) were analyzed from the water samples collected during the 2024 and 2025 campaigns (Table 6).

**Table 6.** TPH values for in-water samples collected in autumn 2024 and summer 2025 from lagoons and river mouths from the tributaries of the Danube. Values highlighted in yellow represent concentrations that exceed the quality standards for sediments as established by national legislation (Order 161/2006)

| **Sampling site (geographical coordinates) /Campaign** | | **Razim 1** | **Razim 2** | **Razim 3** | **Sf. Gheorghe** | **Sulina** | **Chilia** |
|---|---|---|---|---|---|---|---|
| | | **44.685820 28.988257** | **44.606640 28.913545** | **44.790446 29.113935** | **44.886708 29.605545** | **45.165444 29.703541** | **45.310291 29.666798** |
| **TPH (µg/L)** | **2024** | 90 | 90 | - | 100 | 150 | - |
| | **2025** | 210 | 150 | 120 | 100 | 130 | 60 |

The relationship between TPH and the water's chemical matrix is characterized by several key interactions, with TPH exhibiting a moderate to strong positive correlation with both turbidity ($r = 0.567$; $\rho = 0.574$) and pH ($r = 0.535$). Furthermore, positive correlations were observed with zinc ($r = 0.590$; $\rho = 0.555$) and lead ($r = 0.443$; $\rho = 0.464$), associations that often indicate a common source of pollution. Conversely, TPH correlates negatively with cadmium ($r = -0.521$) and nickel ($\rho = -0.440$), an inverse relationship suggesting that factors favoring hydrocarbon persistence might limit the bioavailability or presence of these specific metals in the soluble phase. There is also a moderate negative correlation with conductivity ($r = -0.504$) and chlorides ($r = -0.495$). Water quality and pollutant distribution were assessed using PCA (Table 7) to simplify complex data into its most important patterns. The results reveal a complex structure of variability, where the first five principal components (PC1–PC5) present eigenvalues greater than one, accounting for a significant 89.8% of the total variance in the dataset. The first principal component (PC1) explains 30.5% of the variability, acting as the dominant factor that likely reflects the major anthropogenic impact on the ecosystem. Together with PC2 (22.7%), these two axes define more than half of the chemical dynamics of the analyzed samples (53.2%). The high eigenvalue of the first component (4.26) (Table 7) indicates a strong interdependence between core physico-chemical parameters and the presence of hydrocarbons. The fact that four components are required to exceed the 82.6% threshold of cumulative variance suggests the existence of multiple independent sources of contamination. While the primary components tend to group indicators of organic pollution, the secondary components highlight specific variations in heavy metals and nutrients. This statistical distribution confirms that isolated monitoring of a single parameter is insufficient and necessitates a multivariate approach to fully understand the degradation processes in the studied aquatic environment.

**Table 7.** Eigenanalysis of the Correlation Matrix (PC1-PC10)

| | | | | | | | | | | |
|---|---|---|---|---|---|---|---|---|---|---|
| **Eigenvalue** | 4.2659 | 3.1787 | 2.3708 | 1.7481 | 1.0015 | 0.6479 | 0.4872 | 0.1607 | 0.0966 | 0.0409 |
| **Proportion** | 0.305 | 0.227 | 0.169 | 0.125 | 0.072 | 0.046 | 0.035 | 0.011 | 0.007 | 0.003 |
| **Cumulative** | 0.305 | 0.532 | 0.701 | 0.826 | 0.898 | 0.944 | 0.979 | 0.990 | 0.997 | 1.000 |

From the analysis of physical and chemical parameters, especially chlorides, it appears that the connection between the body of water inside the lagoon and the Black Sea ensures a constant salinity regardless of temperature, which indicates that salt water can penetrate the freshwater body relatively constantly through infiltration. In this case, the oil spill that may reach the coastal area is unlikely to have an impact on the lagoon but is very likely to have an impact along the coastal area, including the Sf. Gheorghe and Sulina estuaries. Thus, the level of petroleum product pollution at a specific time is defined by the following relationship:

$$TPH = f(TPH_{civil}, TPH_{M}) + TPH_{Ev}$$

where: TPH – Total Petroleum Hydrocarbons; $TPH_{civil}$ – Contribution from civilian ships, dependent on the number of ships present in the protected area within a time interval $T \leq 7$ days; $TPH_{M}$ – Contribution from military ships, also dependent on their presence in the protected area within a time interval $T \leq 7$ days; $TPH_{Ev}$ – Contribution from a specific event (e.g., an oil spill due to conflict), influenced by the event's location, timing, and the speed/direction of water currents.

## Conclusions

This study examines the combined effects of civilian and military activities on water and sediment quality in the Razim–Sinoe lagoon complex and the Danube River mouths connected to the Black Sea. The findings indicate distinct seasonal and spatial variations in physico-chemical parameters, heavy metals, and petroleum hydrocarbons, with elevated concentrations of Pb, Ni, Zn, and Fe, particularly in the Chilia area, which is closest to the conflict-affected zone.

Satellite-based analysis confirmed the potential impact of oil spills on protected marine and coastal ecosystems, underscoring the vulnerability of habitats associated with the Danube Delta. While concentrations of several heavy metals in water samples remained below critical thresholds, their accumulation in sediments indicates a risk of long-term ecological effects due to persistence and bioaccumulation. The proposed relationship for Total Petroleum Hydrocarbons (TPH) provides a conceptual framework for estimating petroleum pollution generated by both civilian maritime transport and armed conflict-related activities.

An important aspect highlighted by this study is that the environmental impact of armed conflicts may persist long after the direct events cease, due to the long-term accumulation, transport, and bioaccumulation of contaminants in aquatic ecosystems. The overlap between military-related pollution and existing industrial, domestic, and maritime pressures creates cumulative effects that can significantly influence biodiversity conservation, habitat integrity, and ecosystem resilience in the Black Sea coastal region.

The results highlight the urgent need for targeted measures to conserve natural capital and strengthen ecosystem resilience in the Black Sea coastal and lagoon environments. Recommended actions include developing integrated monitoring systems for water, sediment, and biodiversity quality; maintaining continuous surveillance of oil pollution and heavy metal accumulation; and establishing early-warning mechanisms for accidental or conflict-related contamination events. Special consideration should be given to protected areas and ecologically sensitive habitats connected to the Danube Delta, where cumulative pressures may accelerate habitat degradation and biodiversity loss.

Active management measures should be developed in accordance with sustainability taxonomy principles and supported by comprehensive environmental databases generated through continuous monitoring programs to ensure verification and validation.

**Acknowledgements/Funding**

This work was carried out through the project Black Sea SIERRA—Harnessing complementary curricular preparedness via sustainable management in response to civil and military pollution on the coastline, tributaries, and lagoons in the Black Sea's North, West, and South zones, funded in the European Maritime, Fisheries and Aquaculture Fund (EMFAF) Programme, Call EMFAF-2023-PIA-FLAGSHIP by the European Climate, Infrastructure and Environment Executive Agency (CINEA). Co-funded by the European Union. Views and opinions expressed are, however, those of the author(s) only and do not necessarily reflect those of the European Union or European Climate, Infrastructure, and Environment Executive Agency (CINEA). Neither the European Union nor the granting authority can be held responsible for them.

**References**

[1] M. Strokal, V. Strokal, and C. Kroeze, "The future of the Black Sea: More pollution in over half of the rivers," *Ambio*, vol. 52, no. 2, pp. 339–356, 2023. DOI: 10.1007/s13280-022-01780-6.

[2] D. György et al., "Assessing the Transboundary Water Pollution Possibly Produced By an Armed Conflict," *E3S Web Conf.*, vol. 589, Article Number: 06007, 2024. DOI: 10.1051/e3sconf/202458906007.

[3] V. -M. Manoiu, M. -S. Costache, and M. -A. Nica, "The Impact of the Russia–Ukraine War on Water Resources and Infrastructure of Ukraine—A Comprehensive Review," *World*, vol. 7, no. 1, Article Number: 3, 2026. DOI: 10.3390/world7010003.

[4] F. Marinescu *et al.*, "Ecological risk assessment of heavy metals in surface sediments from the Danube River," *Carpathian J. Earth Environ. Sci.*, vol. 12, pp. 437-445, 2017.

[5] G. Y. Deak et al., "Health-environment relation: A key issue of Romanian environmental protection," *J. Environ. Prot. Ecol.*, vol. 16, no. 1, pp. 304–315, 2015.

[6] M. Devlin and J. Brodie, "Nutrients and eutrophication," in *Marine Pollution – Monitoring, Management and Mitigation*, A. Reichelt-Brushett, Ed. Cham, Switzerland: Springer Nature Switzerland, 2023, pp. 75–100, 2023. DOI: 10.1007/978-3-031-10127-4_4.

[7] M. Ilie, G. Ghita, G. Deak, A. -M. Anghel, and M. Raischi, "Spatial distribution of water quality and eutrophication levels of Divici-Pojejena wetlands," in *Proc. SGEM 2016 Int. Multidisciplinary Sci. GeoConf.*, Book 3, pp. 267–274, 2016. DOI: 10.5593/SGEM2016/HB33/S02.034.

[8] D. D. Burduhos Nergis, P. Vizureanu, G. Deak, G. Tudor, and A. V. Sandu, "Intelligent filtration method for marine pollution decontamination," *Int. J. Conserv. Sci.*, vol. 16, no. 4, pp. 1993–2002, 2025. DOI: 10.36868/IJCS.2025.04.26.

[9] M. Mityagina and O. Lavrova, "Satellite survey of inner seas: Oil pollution in the Black and Caspian Seas," *Remote Sens.*, vol. 8, no. 10, Article Number: 875, 2016. DOI: 10.3390/rs8100875.

[10] S. Kyrii, M. Litynska, and A. Misevych, "The war impact on Ukraine's marine environment," *Water Water Purif. Technol. Sci. Tech. News*, vol. 38, no. 1, pp. 37–46, 2024. DOI: 10.20535/2218-930012024316112.

[11] X. Yu, W. Feng, F. Song, Y. Han, Q. Miao, and J. M. Gonçalves, "Characterisation of heavy metals and microbial communities in urban river sediments: Interactions and pollution origin analysis," *Environ. Res.*, vol. 280, Article Number: 121925, 2025. DOI: 10.1016/j.envres.2025.121925.

[12] L. O. Ajala, J. E. H. Wilson, M. Jiru, and M. O. Iwunze, “Perspective on health and ecological risk assessments of potentially toxic metal(loid)s using aquatic biodiversity as biomonitoring indicators,” *Toxicol. Rep.*, vol. 15, Article Number: 102086, 2025. DOI: 10.1016/j.toxrep.2025.102086.
[13] K. Peng, C. Luo, L. Lou, X. Li, and Z. Shen, “Bioaccumulation of heavy metals by the aquatic plants Potamogeton pectinatus L. and Potamogeton malaianus Miq. and their potential use for contamination indicators and in wastewater treatment,” *Sci. Total Environ.*, vol. 392, no. 1, pp. 22–29,2008. DOI: 10.1016/j.scitotenv.2007.11.032.
[14] J. X. Lv, R. J. Hu, N. Wang, L. G. Zhu, X. D. Zhang, X. D. Yuan, B. Liu, “Distribution and movement of heavy metals in sediments around the coastal areas under the influence of multiple factors: A case study from the junction of the Bohai Sea and the Yellow Sea,” *Chemosphere,* vol. 278, Article Number: 130352, 2021. DOI: 10.1016/j.chemosphere.2021.130352.
[15] A. Mussakulkyzy, C. Opp, N. Amirgaliev, A. Madibekov, L. Ismukhanova, and A. Zhadi, “Transmission of heavy metals in river water and self-purification capacity of Ile River,” *Appl. Sci.*, vol. 15, no. 12, Article Number: 6548, 2025. DOI: 10.3390/app15126548.
[16] A. Oros, “Bioaccumulation and trophic transfer of heavy metals in marine fish: Ecological and ecosystem-level impacts,” *J. Xenobiotics*, vol. 15, no. 2, Article Number: 59, Apr. 2025, doi: 10.3390/jox15020059.
[17] S. R. de Solla, “Exposure, bioaccumulation, metabolism and monitoring of persistent organic pollutants in terrestrial wildlife,” in *Dioxin and Related Compounds*, vol. 49, M. Alaee, Ed., ser. *The Handbook of Environmental Chemistry*. Cham, Switzerland: Springer, pp. 203–252, 2015. DOI: 10.1007/698_2015_450.
[18] D. Hryhorczuk *et al.*, “The environmental health impacts of Russia’s war on Ukraine,” *J. Occup. Med. Toxicol.*, vol. 19, no. 1, Article Number: 1, 2024, doi: 10.1186/s12995-023-00398-y.
[19] A. Oros, V. Coatu, N. Damir, D. Danilov, and E. Ristea, “Recent findings on the pollution levels in the Romanian Black Sea ecosystem: Implications for achieving good environmental status (GES) under the Marine Strategy Framework Directive (Directive 2008/56/EC),” *Sustainability*, vol. 16, no. 22, Article Number: 9785, 2024. DOI: 10.3390/su16229785.
[20] “Copernicus Browser,” Copernicus Browser. Accessed: May 27, 2026. [Online]. Available: https://browser.dataspace.copernicus.eu/
[21] “STEP – Science Toolbox Exploitation Platform.” Accessed: May 27, 2026. [Online]. Available: https://step.esa.int/main/
[22] Nyall Dawson *et al.*, *qgis/QGIS: 4.0.2*. (May 01, 2026). Zenodo.
[23] T. Metsalu and J. Vilo, “ClustVis: A web tool for visualizing clustering of multivariate data using Principal Component Analysis and heatmap,” *Nucleic Acids Res.*, vol. 43, no. W1, pp. W566–W570, 2015. DOI: 10.1093/nar/gkv468.
[24] “Analytics Solutions for Data Analysis & Process Improvement,” Minitab. Accessed: May 27, 2026. [Online]. Available: https://www.minitab.com/en-us/
[25] I. Jolliffe, “Principal component analysis,” in *International Encyclopedia of Statistical Science*, M. Lovric, Ed. Berlin, Heidelberg: Springer, 2025, pp. 1945–1948, 2025. DOI: 10.1007/978-3-662-69359-9_483.
[26] S. K. Dewangan, S. K. Shrivastava, V. Tigga, M. Lakra, Namrata, and Preeti, “Review paper on the role of pH in water quality: Implications for aquatic life, human health, and environmental sustainability,” *Int. Adv. Res. J. Sci. Eng. Technol.*, vol. 10, no. 6, pp. 215–218, 2023. DOI: 10.17148/IARJSET.2023.10633.
[27] P. Luo et al., “Nitrogen removal and recovery from lagoon-pretreated swine wastewater by constructed wetlands under sustainable plant harvesting management,” *Bioresour. Technol.*, vol. 258, pp. 247–254, 2018. DOI: 10.1016/j.biortech.2018.03.017.

[28] X. Chen et al., "Cold temperature increases nitrate accumulation in pilot-scale surface flow constructed wetlands with high rates of nitrogen removal," *Agric. Ecosyst. Environ.*, vol. 308, Article Number: 107250, 2021. DOI: 10.1016/j.agee.2020.107250.
[29] B. M. Saalidong, S. A. Aram, S. Otu, and P. O. Lartey, "Examining the dynamics of the relationship between water pH and other water quality parameters in ground and surface water systems," *PLOS ONE*, vol. 17, no. 1, Article Number: e0262117, 2022. DOI: 10.1371/journal.pone.0262117.
[30] B. M. Saalidong, S. A. Aram, S. Otu, and P. O. Lartey, "Examining the dynamics of the relationship between water pH and other water quality parameters in ground and surface water systems," *PLOS ONE*, vol. 17, no. 1, p. e0262117, 2022.
[31] A. Alkan, S. Serdar, D. Fidan, U. Akbas, B. Zengin, and M. B. Kilic, "Physico-chemical characteristics and nutrient levels of the Eastern Black Sea rivers," *Turk. J. Fish. Aquat. Sci.*, vol. 13, no. 5, pp. 847–859, 2013. DOI: 10.4194/1303-2712-v13_5_09.
[32] *Order 161/20206, Regulation on the classification of surface water quality to establish the ecological status of water bodies from 16.02.2006*, Feb. 16, 2006.
[33] P. Zhang et al., "Water quality degradation due to heavy metal contamination: Health impacts and eco-friendly approaches for heavy metal remediation," *Toxics*, vol. 11, no. 10, Article Number: 828, 2023. DOI: 10.3390/toxics11100828.
[34] K. Gębka, J. Bełdowski, and M. Bełdowska, "The impact of military activities on the concentration of mercury in soils of military training grounds and marine sediments," *Environ. Sci. Pollut. Res*., vol. 23, no. 22, pp. 23103–23113, 2016. DOI: 10.1007/s11356-016-7436-0.
[35] A. Oros, D. Marin, G. Reiz, and R. D. Nenita, "Tracing heavy metal pollution in the Romanian Black Sea: A multi-matrix study of contaminant profiles and ecological risk across the continental shelf and beyond," *Water,* vol. 17, no. 16, Article Number: 2406, 2025. DOI: 10.3390/w17162406.
[36] A. A. Jimoh, S. O. Azeez, and W. Jamiu, "Recent developments in heavy metal remediation from polluted water: Sources, environmental impacts, and sustainable hybrid treatment strategies," Discov. Chem., vol. 3, Article Number: 279, 2026. DOI: 10.1007/s44371-026-00721-6.
[37] M. I. Litynska and O. B. Pelekhata, "The influence of the war on the content of some components in the rivers of Ukraine," *IOP Conf. Ser. Earth Environ. Sci.*, vol. 1415, no. 1, Article Number: 012094, 2024. DOI: 10.1088/1755-1315/1415/1/012094.
[38] S. Kyrii, M. Litynska, and A. Misevych, "The war impact on Ukraine's marine environment," *Water Water Purif. Technol. Sci. Tech. News*, vol. 38, no. 1, pp. 37–46, 2024. DOI: 10.20535/2218-930012024316112.
[39] S. Boichenko, K. Lejda, O. Lychmanenko, M. Boichenko, and V. Reshetilowski, "Modification of aviation gasoline with aliphatic alcohols additives: An analytical review of prospects," *Int. J. Sustain. Aviat.*, vol. 1, no. 4, pp. 324–332, 2015. DOI: 10.1504/IJSA.2015.074734.
[40] A. Oros, V. Coatu, N. Damir, D. Danilov, and E. Ristea, "Recent findings on the pollution levels in the Romanian Black Sea ecosystem: Implications for achieving good environmental status (GES) under the Marine Strategy Framework Directive (Directive 2008/56/EC)," *Sustainability*, vol. 16, no. 22, Article Number: 9785, 2024. DOI:10.3390/su16229785.
[41] J.A. Tørnes and G.P. Novik, "Evaluating the environmental impact of leaking WW2 shipwrecks: A closer look at the VRAKA and AmuCad decision support tools," *Mar. Pollut. Bull.,* vol. 215, Article Number: 117930, 2025. DOI: 10.1016/j.marpolbul.2025.117930.

*Received: June 12, 2026*
*Accepted: September 10, 2026*